Dominant Partial Waves for the Reaction $^{28}Si(^{16}O,^{12}C)^{32}S$ and Entrance and Exit Channel Elastic Scattering

T. Awes, J. Barrette,* U.E.P. Berg, P. Braun-Munzinger,** C.K. Gelbke, and M.J. LeVine*

Recently, resonant structures[1,2] have been observed in backward-angle excitation functions for the elastic and inelastic scattering of ^{12}C and ^{16}O on ^{28}Si. Similar structures have also been seen in the forward[3] as well as backward-angle[4] excitation functions of the α-transfer reaction $^{24}Mg(^{16}O,^{12}C)^{28}Si$. These observations are at present not understood. In particular, it is uncertain whether these resonances are associated with structure in the compound nucleus and how the partial waves responsible for the resonances in the elastic channels relate to the partial waves dominating the transfer channels. In order to gain more insight into these problems we have measured the backangle elastic excitation function for the system $^{12}C+^{32}S$, as well as the angular distributions of the reaction $^{28}Si(^{16}O,^{12}C)^{32}S$ and the entrance and exit channel elastic scattering at E_{cm} ($^{16}O+^{28}Si$) = 26.2 MeV.

The experiment was performed at the tandem Van de Graaff facility of the Brookhaven National Laboratory, using the technique described in Ref. 5. The elastic scattering excitation functions of entrance and exit channel are shown in Fig. 1 (data for $^{16}O+^{28}Si$ from Ref. 1). No obvious

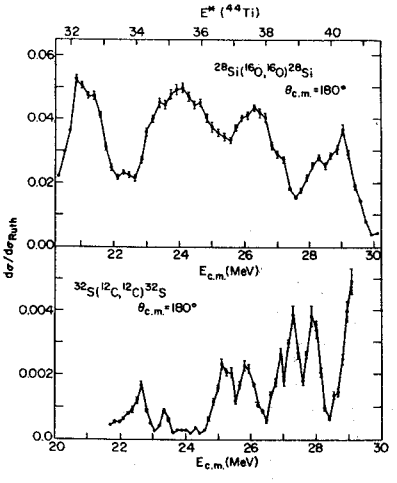

Fig. 1

correlations are observed between the gross structures observed in both systems, indicating that the resonance-like phenomena are not generated by a common doorway state in the compound nucleus.

The angular distributions are shown in Fig. 2; they exhibit pronounced structures and a strong rise at backward angles. The solid curves are calculations using a Regge parametrization[5] for the S-matrix element for the partial wave ℓ

$$S_\ell = S_\ell^o \left(1 + i \frac{D_\ell\, e^{2i\phi}}{\ell-\ell_o-i\Gamma/2}\right) \qquad (1)$$

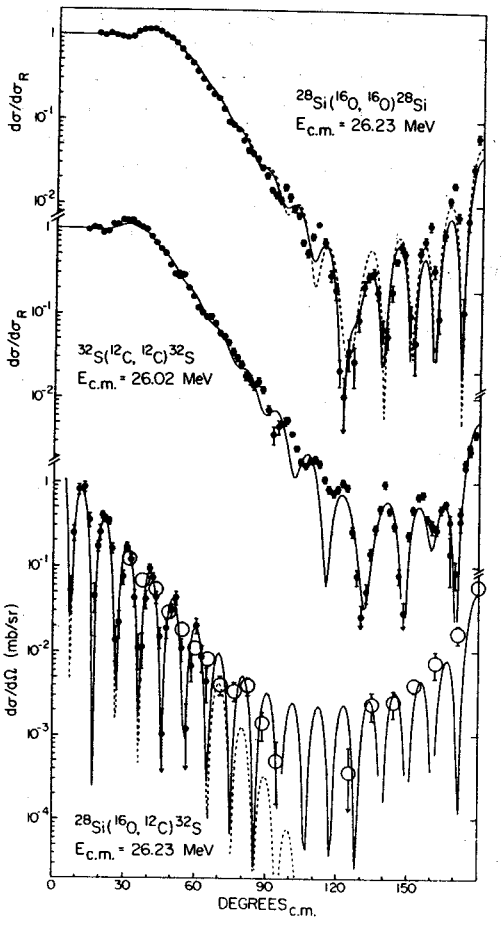

Fig. 2

In the case of elastic scattering, S_ℓ is the nuclear part of the elastic S-matrix, the background S_ℓ^o has been calculated using potential E18 of Ref. 6 and the elastic width has been taken as[5] $D_\ell=D_o(1-|S^o|)$. In the case of transfer, S_ℓ is the transfer matrix element and $D_\ell=D_o$ is the transfer width. The background S_ℓ^o (represented by the dashed line) has been parametrized as[7]

$$S_\ell^o = \exp\left(2i\theta_o\ell - (\ell-\ell_1)^2/\Delta^2\right) \qquad (2)$$

using $\theta_o=2^o$, $\Delta=2.3$, and $\ell_1=17.9$. The pole parameters are listed in Table I (of course, they are not determined for the transfer case--this will require further measurements). Different partial waves dominate the backangle elastic scattering of entrance and exit channel. Consequently, the resonant structures observed in the elastic channels are not due to a common doorway state in the compound nucleus, as was already inferred from the excitation function. Instead, they appear to depend on the reaction channel. The

fact that higher partial waves (ℓ_1=17.9) than the elastic poles (ℓ_o=16.06 and 14.85) dominate the transfer reaction at forward angles is not expected from from the Regge pole model for transfer reactions,[8] in terms of which a consistent description was not possible.

---

* Brookhaven National Laboratory, Upton, NY.
** S.U.N.Y., Stony Brook, NY.

1. J. Barrette et al., Phys. Rev. Lett. 40 (1978) 445.
2. M.R. Clover et al., Phys. Rev. Lett. 40 (1978) 1008.
3. M. Paul et al., Phys. Rev. Lett. 40 (1978) 1310.
4. P. Chevalier, et al., Tokyo Conference 1977.
5. P. Braun-Munzinger et al., Phys. Rev. Lett. 38 (1977) 944.
6. J.G. Cramer et al., Phys. Rev. C 14 (1976) 2158.
7. V.M. Strutinsky, Sov. Phys. JETP 19 (1964) 1401.
8. R.C. Fuller et al., Phys. Rev. Lett. 32 (1974) 617.

Table I.

Channel	ℓ_0	Γ	D_0	ϕ
$^{16}O+^{28}Si$, elastic	16.06	0.13	0.026	45°
$^{12}C+^{32}S$, elastic	14.85	1.7	0.7	90°
$^{28}Si(^{16}O,^{12}C)^{32}S$	16.06	0.13	0.07	0°

Sequential Fission in Peripheral Reactions of 20 MeV/A ^{16}O with ^{238}U

P. Dyer, C.K. Gelbke, T.C. Awes, B.B. Back,* A. Mignerey,*
H. Breuer,+ V.E. Viola,+ W.G. Meyer,++ and K.L. Wolf++

Reactions between ^{16}O and heavy nuclei for ^{16}O bombarding energies below about 10 MeV/nucleon are dominated by fusion and grazing collisions (including transfer reactions and deeply inelastic collisions). At higher energies, different mechanisms for energy, momentum, and mass transfer, such as nucleon-nucleon collisions and fragmentation, become important.[1]

We have begun a study of the reaction mechanisms for 11 and 20 MeV/nucleon ^{16}O incident on ^{238}U and ^{197}Au targets, where the emphasis of the first experiment, conducted at the LBL 88" cyclotron, has been on the linear momentum transfer. We have measured coincidences between two fission fragments, with and without a coincidence with a light product (Z=2 to 8). Targets of 200 $\mu g/cm^2$ UF_4 on a 50 $\mu g/cm^2$ carbon backing and of 300 $\mu g/cm^2$ gold were bombarded by ^{16}O beams of energies 215 and 315 MeV and intensities of up to 10 nA. Fission fragments were detected by two position-sensitive solid-state detectors placed in the reaction plane on each side of the beam, each subtending 35^o. Light products were detected at 15^o (lab), near the grazing angle, by a three-element solid-state telescope, which allowed Z and A identification.

In Fig. 1(a) we show the fission yield for 315-MeV ^{16}O on ^{238}U as a function of the angle between the two fission fragments $\Delta\theta$ (in the lab frame of reference) for measurements in which no coincidence with a light product was required. This angle difference $\Delta\theta$ is a measure of the linear momentum along the beam direction of the fissioning nucleus. An approximate momentum scale is given on the plot. The distributions are made up of many components. If complete fusion occurs, and the compound nucleus fissions, $\Delta\theta$ will be about 144^o, with a range of magnitudes indicated "CN" on the plot. If one or more particles are emitted from the compound system before fission takes place, $\Delta\theta$ will be centered about the same angle if the emission is isotropic in the center of mass (although the distribution will be broader), but $\Delta\theta$ will increase if the particles are emitted preferentially forward (along the beam direction). In the limit that zero momentum is transferred to the target, $\Delta\theta$ is 180^o.

The curves in Figs. 1(b) through 1(h) are smooth curves drawn through the data obtained from 315-MeV ^{16}O + ^{238}U by requiring a coincidence with particles of various Z's detected by the telescope. (Events for all kinetic energies are summed, but the requirement thus far that pulses be present in all three telescope detectors eliminates some of the Z=2 and Z=8 events.) Heavier products, such as ^{16}O, leave the residual nucleus with the least amount of forward momentum and the $\Delta\theta$ distributions peak at larger $\Delta\theta$. By studying carefully the distributions for the individual Z's, it is possible to determine whether the unobserved mass is transferred to the target, emitted forward, or emitted in some other direction. For example, if a ^{12}C particle is detected, the missing alpha particle may have been transferred to the residual nucleus, and the fission event would be characterized by a relatively small $\Delta\theta$. If the alpha particle is emitted forward, less linear momentum is transferred, and $\Delta\theta$ will be larger. For Z=6, there is little difference in $\Delta\theta$ for these two cases; however, for Z=2 there is a large difference. There is some evidence that the Z=2 data has two components: one for the missing Z=6 transferred to the target (smaller $\Delta\theta$), and one for the missing Z=6 being emitted forward (larger $\Delta\theta$). This second component has an average $\Delta\theta$ about the same as that of the Z=6 data. We are presently examining this three-fold coincidence data in detail, comparing the distributions with those expected on the basis of different amounts of momentum transfer. The preliminary analysis indicates that the average momentum transferred to the target is halfway between that corresponding to a simple transfer reaction and that of projectile breakup.

Further studies of this data (plus additional data from fission fragments detected out of the reaction plane, planned for the next experiment) can also provide information about transfer of kinetic energy to internal degrees of freedom, through studies of fission probabilities with ^{197}Au and ^{238}U targets and studies of mass asymmetries with the ^{238}U target.

---

* Argonne National Laboratory, Argonne, IL.
+ University of Maryland, College Park, MD.
++ Lawrence Berkeley Laboratory, Berkeley, CA.

1. C.K. Gelbke, C. Olmer, M. Buenerd, D.L. Hendrie, J. Mahoney, M.C. Mermaz, and D.K. Scott, Physics Reports, in press.

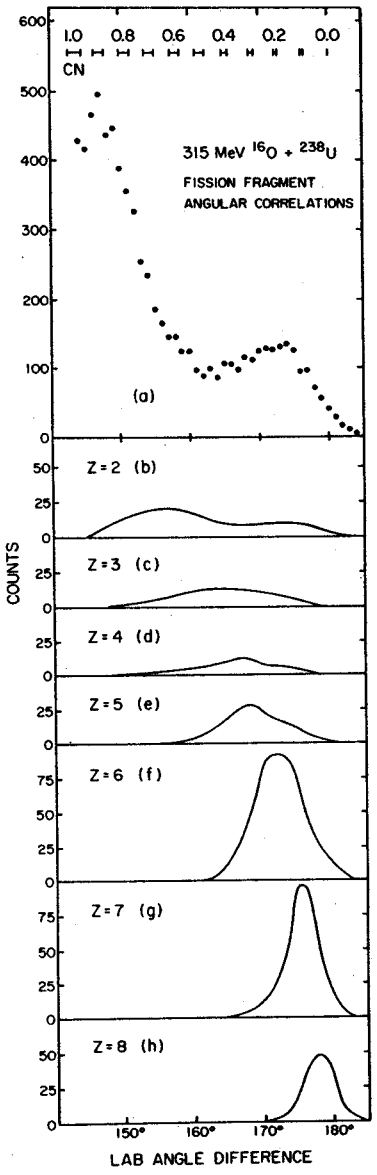

Fig. 1. Fission yields as a function of the (lab) angle between the two fission fragments with no light-product coincidence required (a) and with coincidences required for varying Z of the light product {(b) through (h)}. The approximate amount of forward momentum of the fissioning nucleus $P_{||}$ relative to that of the beam P_0 is indicated by an additional scale. The label "CN" indicates the range of angles for complete linear momentum transfer.

Pion Production Near Threshold in Heavy Ion Collisions

G.M. Crawley, W. Benenson, G. Bertsch, E. Kashy, J.A. Nolen, Jr., J.O. Rasmussen,* H. Bowman,* M. Sasao,* J. Ioannou,* M.C. Lemaire,*+ J. Sullivan,* L. Oliveira,* M. Koike,++ and J. Chiba++

The production of pions in heavy ion collisions near threshold is an extremely interesting problem, both theoretically and experimentally. According to current theoretical ideas on pion-nucleon interactions, nuclear matter is not far from a phase transition involving the pion field. Models for the behavior of the pion in nuclear matter show peculiarities such as a near-zero or negative effective mass for the pion.[1] Under such such conditions, pions can be produced in the interactions of nucleons with the potential field,[2] in addition to production in the collisions of nucleons with each other. The rate of pion production is thus increased by the potential field mechanism, and a characteristic angular distribution is predicted for the pions.

On the experimental side, the information on the pion production cross section at energies near threshold, obtained using emulsions, is conflicting. In one case a very high pion multiplicity per collision is reported,[3] but in the other cases[4,5] a much lower upper limit for pion production is given. A theoretical prediction has been made for this cross section, based on production by nucleon-nucleon collisions alone.[6]

In the present experiment, measurements were made with 400 MeV/A and 250 MeV/A Argon beams from the Berkeley Bevalac incident on KCl and Pb targets. Pions were detected near 0° using plastic scintillator telescopes in a 180° magnetic spectrograph set up specifically for these measurements. A preliminary analysis of the data from the first run shows that the π^+ yield at 250 MeV/A is about a factor of three of four lower than at 400 MeV/A for the KCl target (see Fig. 1). The present data are consistent with the lower limit established by Lindstrom et al.[4] and Kullberg et al.[5] and disagree with the earlier measurements.[3]

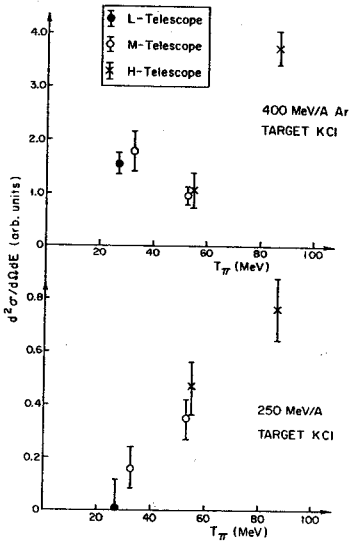

Fig. 1. Cross sections from preliminary run with 400 MeV/A and 250 MeV/A Argon beam on a KCl target.

---

* Lawrence Berkeley Laboratory, University of California, Berkeley, CA 94720.
+ On leave from C.E.N., Saclay.
++ University of Tokyo.

1. G. Bertsch and N. Johnson, Phys. Rev. D 12 (1975) 2230.
2. R. Sawyer, Nucl. Phys. A271 (1976) 235.
3. P.J. McNulty et al., Phys. Rev. Lett. 38 (1977) 1519.
4. P. Lindstrom et al., Phys. Rev. Lett. 40 (1978) 93.
5. R. Kullberg et al., Phys. Rev. Lett. 40 (1978) 289.
6. D. Malbrough et al., Los Alamos preprint LA-UR-77-1939.

Nucleon Tunnelling Model of Mass Diffusion in Deep Inelastic Heavy Ion Collisions

C.M. Ko, G.F. Bertsch, and D. Cha

The transfer of nucleons in deep inelastic heavy ion collisions was first described successfully by Nörenberg[1] as a diffusion process. Many people have since attempted to determine the mass diffusion coefficient both theoretically and phenomenologically. Among them, Randrup[2] has proposed a proximity formalism to approximate the mass flux in the nuclear Thomas-Fermi approximation. Unlike Randrup, we calculate the flux from the quantum mechanical barrier penetration.

For simplicity, we consider a one-dimensional geometry neglecting completely the effect of angular momentum. We describe the two ions by the Fermi gas model and neglect the single-particle Coulomb potential. We take the average single-particle potential as a Woods-Saxon well characterized by the three parameters; depth V_o, radius R, and thickness a. Then the combined potential felt by the nucleons, when the two ions are separated by the distance s measured between the half potential points, is given by:

$$V(x,s) = Vo - \frac{Vo}{1+\exp\frac{|x+R_1+0.5s|-R_1}{a}} - \frac{Vo}{1+\exp\frac{|x-R_2-0.5s|-R_2}{a}}$$

With this potential the transmission probability $P(k_x,s)$ for a nucleon in first well with momentum $\hbar k_x$ in the x-direction tunnelling through the barrier to the second well can be obtained by numerically solving the one-dimensional Schrödinger equation.

Using a diffuse Fermi surface characterized by a temperature T, the total flux transmitted is given by:

$$\phi(s) = \frac{T}{\pi^2\hbar}\int_0^\infty dk_x\, P(k_x,s)\; k_x\, \ln\{1+\exp[(\frac{\hbar^2}{2m}(k_F^2-k_x^2)/T)\}$$

where m is the nucleon mass, and k_F is the Fermi momentum and has the value 1.36 fm^{-1}. Taking V_o=50 MeV and a=0.6 fm in consistence with the shell-model potential, the T dependence of $\phi(s)$ is negligible for physically significant distance s=0-2 fm. It is seen that $\phi(s)$ can be reasonably approximated by:

$$\phi(s) = \alpha_1 e^{-\beta_1 s} + \alpha_2 e^{-\beta_2 s}$$

$$\alpha_1 = 0.027\ c\cdot fm^{-3}, \qquad \alpha_2 = -0.018\ c\cdot fm^{-3}$$

$$\beta_1 = 1.90\ fm^{-1}, \qquad \beta_2 = 2.98\ fm^{-1}$$

Assuming that nucleon transfers are statistical, then the mass diffusion coefficient can be obtained from the rate of nucleon transferred by integrating $\phi(s)$ over the facing surfaces of the two ions, i.e.

$$D_A = 2\pi \frac{R_1 R_2}{R_1+R_2}\left\{\frac{\alpha_1}{\beta_1} e^{-\beta_1 s} + \frac{\alpha_2}{\beta_2} e^{-\beta_2 s}\right\}$$

In order to compare with the empirical values, we assume that nucleon exchanges occur when the two ions are in contact at s=0 fm. Using $R=1.25 \times A^{1/3}$ for the radius, where A is the mass number, we obtain Table I. We observe that our predictions are systematically larger than those predicted by Nörenberg et al.[4] Our results agree with experiment better for the heavier systems, but not as well for the lighter systems, being off by a factor two. This is perhaps as good as can be expected for a model which does not treat the relative motion.

1. W. Nörenberg, Phys. Lett. B52 (1974) 289.
2. J. Randrup, NORDITA preprint (1978).
3. G. Wolschin and W. Nörenberg, Z. Phys. A284 (1978) 209.
4. S. Ayik, B. Schurmann, and W.Nörenberg, Z. Phys. A277 (1976) 299, A279 (1976) 145.

Table I. Empirical and theoretical values for the mass diffusion coefficients in units of 10^{22} $sec.^{-1}$.

Reaction	E_{lab}(MeV)	D_Ath (Ko et al.)	D_Ath Nörenberg et al.)	D_A (Empirical ref. 3)
$^{40}Ar + ^{108}Ag$	288	3.0	1.63	1.3
$^{86}Kr + ^{197}Au$	620	3.7	2.43	2.0
$^{84}Kr + ^{165}Ho$	714	3.6	2.40	2.4
$^{84}Kr + ^{209}Bi$	714	3.8	2.48	3.7
$^{136}Xe + ^{209}Bi$	1130	4.1	2.83	4.0

Role of Deformation in Deep Inelastic Heavy Ion Collisions

C.M. Ko

A unique feature of deep inelastic heavy ion collisions is the existence of a low energy peak in the cross section, usually at energy below the Coulomb energy of two touching spherical nuclei. Deubler and Dietrich[1] were the first to suggest that such phenomena are due to deformations of the ions in the exit channel.

In the work of Agassi, Ko, and Weidenmüller,[2] a transport equation is derived for the phase space probability function of the relative motion. Many features of the experimental data are reproduced in the transport theory. However, due to the neglect of deformation degree of freedom, they are unable to reproduce the low energy peak in the cross sections.

Recently we have shown that collective excitations, such as shape oscillations and giant resonances, can be consistently incorporated in the transport theory.[3] Explicitly, the deformation of the ion is described by a forced damped harmonic motion

$$\frac{d^2\alpha_i}{dt^2} + \frac{2\,\Gamma_i}{\hbar}\frac{d\alpha_i}{dt} + \left[\omega_i^2 + \left(\frac{\Gamma_i}{\hbar}\right)^2\right]\alpha_i = \frac{-1}{D_i}\frac{\partial V_o(r,\alpha_i)}{\partial \alpha_i}$$

$$i=1 \text{ (projectile)},\ 2 \text{ (target)}$$

where α_i describes the surface deformation of the ions, i.e.

$$R_i(\theta_i) = R_i^{(o)}\,[1 + \alpha_i\ P_2\ (\cos\theta_i)]$$

In the above equation, $R_i^{(o)}$ denotes the radius of the ion at spherical shape and θ_i measures the angle with respect to its symmetry axis. Also, we restrict ourselves to quadrupole deformations only. The frequency ω_i is defined to be $(C_i/D_i)^{1/2}$ with C_i and D_i the stiffness and inertia parameters, respectively. The damping factor is denoted by Γ_i, while the ion-ion potential is given by $V_o\ (r,\alpha_i)$.

We have applied the model to study the reaction $^{136}Xe + {}^{209}Bi$ at E_{lab} = 1130 MeV. The same statistical inputs as in Ref. 2 are used. The Coulomb potential and the nuclear proximity potential are generalized to deformed nuclei. The stiffness and inertia parameters C_i and D_i are taken from the liquid-drop model. Very little is known about the damping factor Γ_i; we therefore use $\Gamma_i = 0.5\,\hbar\omega_i$ as a rough estimate so that the quadrupole vibration is damped. We have calculated the triple cross sections of angle, energy, and charge. Much improved results over those of ref. 2 are obtained. In particular, the low energy peak in the cross section is clearly exhibited. In Fig. 1, we show the differential cross section as a function of energy loss integrated over all charges and angles. The solid curve is from experiment.[4] Our calculated result is given by the long dashed curve. If the deformation degree of freedom is neglected, then we obtain the short dashed curve in which the low energy peak is missing completely. The fact that the calculated quasielastic peak is too wide in comparison with the experiment could indicate that a more microscopic treatment of the initial states of the reaction is needed.

1. H.H. Deubler and K. Dietrich, Nucl. Phys. A277 (1977) 493.
2. D. Agassi, C.M. Ko, and H.A. Weidenmüller, Ann. of Phys. 107 (1977) 140 and in press, Phys. Lett. 73B (1978) 284.
3. C.M. Ko, Z. Phys. in press.
4. W.U. Schröder et al., Proc. of the Int. Workshop on Gross Properties of Nuclei and Nuclear Exc. VI, Hirschegg, (1978), p. 85.

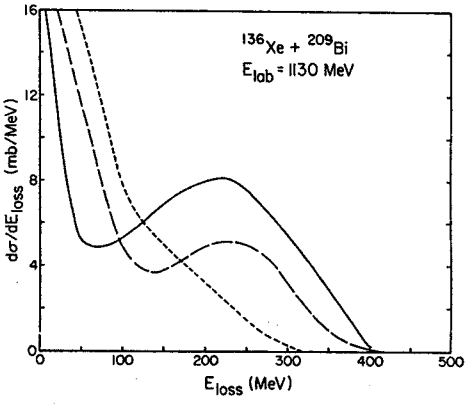

FIG. 1. Integrated energy-loss spectrum. Solid curve is from the experiment, long dashed curve is from the present calculation, and short dashed curve is from the calculation of ref. 2 without deformation degree of freedom.

Intermediate Energy Heavy Ion Collisions

G. Bertsch

At energies above ≃25 MeV/nucleon, heavy ion collisions will cause fragmentation of the colliding nuclei. In order to get useful information about the behavior of the system during the collision, it is important to design experiments which will select out collisions of different impart parameters. It is essential to detect many particles at once; the experience with relativistic heavy ion collisions has shown that inclusive experiments are not sufficient to distinguish different models. If the distribution in momentum of all the products of the collision could be measured, it should be possible to analyze this data in a way that would clearly distinguish different theories and would provide some information on the compressibility of nuclear matter. The impact parameter of the collision would be characterized by the longitudinal component of kinetic energy of the fragments. The longitudinal energy is defined as:

$$E_{||} = \Sigma_i \frac{P_{||}^{L(i)}}{2m_i}$$

We expect at intermediate energies that the smaller the impact parameter, the smaller would be $E_{||}$.

We have computed predictions for $E_{||}$ in the hydrodynamic model. The distribution is shown in Fig. 1 for a collision of two nuclei at 400 MeV/A (lab). The greatest energy loss corresponds to a head-on collision; there is a large cross section for peripheral collisions with relatively small energy loss. The minimum $E_{||}$ is quite sensitive to the model. Hydrodynamics predicts a splashing with $E_{||}$ close to zero for head-on collisions. Mean field models would predict much less energy loss, and in fact the greatest energy loss may be for noncentral collisions.

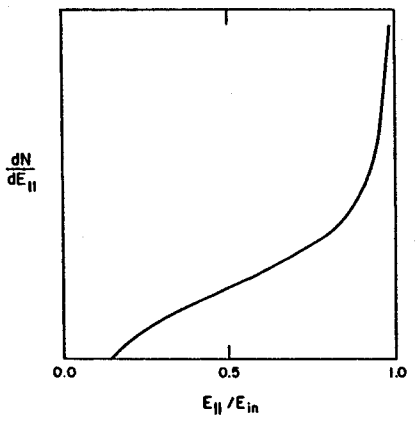

Fig. 1

Other useful quantities to be extracted from the data are coefficients of a spherical harmonic expansion of the cm angular distribution of the products,

$$f(\theta,\phi) \simeq Y_o + \sum_{M}^{L>o} \alpha_{LM} Y^L_M(\theta,\phi)$$

The coefficient of the L=2 M=±1 terms should be sensitive to the compressibility of nuclear matter, since it is just these terms that give the average deflection of nuclei passing through each other in an off-center collision. The α_{21} coefficient for the hydrodynamic collision is shown in Fig. 2. We see that it peaks at $b \simeq 0.46_{max}$. In mean field theory, the maximum α_{21} will be much less.

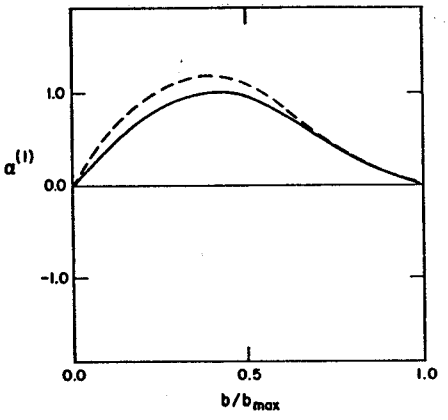

Fig. 2

Experimentally, what would be measured would be a differential cross section $\frac{d\sigma}{dE_{||}\,d\alpha}$. If the statistics of the individual collisions are sufficiently good, there will be a ridge defined in this plot that ought to be reproducible in a classical theory that suitably interpolated between hydrodynamics and mean field dynamics.

Classical Description of Heavy Ion Collisions at Intermediate Energy

G. Bertsch and D. Mundinger

To gain an understanding of how observables in heavy ion collisions at intermediate energy will depend on the underlying nuclear dynamics, we are studying the transport of mass, momentum, and angular momentum for three-dimensional heavy ion collisions. We assume that the transport of these quantities behaves as in a Fermi gas, and we divide the system into regions of normal density and regions that are compressed or rarified. The boundaries between the regions are allowed to change with time in a manner consistent with the conservation laws and Fermi gas fluxes. So far we have studied mostly the threshold for immediate breakup. This threshold appears to be the same for head-on collisions as for the collisions of slabs. The threshold becomes very small for grazing collisions, as expected.

Thermalization of Nuclear Matter in Heavy Ion Collisions

G. Bertsch

An important issue in the theory of heavy ion collisions at intermediate energies is the relative importance of the mean field and of nucleon-nucleon collisions in the dynamics. We therefore examined the collision integral for an infinite Fermi system having a deformed Fermi surface. This simulates the nucleon distribution for interpenetrating nuclei. An interesting conclusion we find is that the only important variable is the internal energy of the system. For a given internal energy, the collision rate is nearly independent of temperature. With reasonable values assumed for nucleon-nucleon cross sections, the collision damping time is much greater than the transit time of the nuclei, for low energy collisions. This implies that the mean field model should be good, and that colliding nuclei are rather transparent to each other.